Southwest Pacific Ocean Water-Mass Changes between 1968/69 and 1990/91*,†

GREGORY C. JOHNSON

NOAA/Pacific Marine Environmental Laboratory, Seattle, Washington

ALEJANDRO H. ORSI

Joint Institute for Study of the Atmosphere and Ocean, University of Washington, Seattle, Washington

(Manuscript received 6 November 1995, in final form 9 July 1996)

ABSTRACT

Water-mass changes are estimated in the southwest Pacific Ocean by comparing a meridional hydrographic section along 170°W between 60°S and the equator occupied in 1968/69 during the Southern Cross cruise and again in 1990 during a NOAA Climate and Global Change cruise. Another comparison is made using a hydrographic section along 35°S between the date line and 169°W occupied in 1969 during USNS *Eltanin* cruise 40 and again in 1991 during a Mapkiwi cruise. The most robust change consists of cooling (and freshening) on isopycnals, with peak differences exceeding −1.0°C (−0.25 pss) at the base of the subtropical thermocline. The cooling and freshening starts above the stratification minimum of the Subantarctic Mode Water and persists to below the salinity minimum of the Antarctic Intermediate Water. Amplitudes are largest at 48°S, near where these water masses subduct, and decay toward 20°S, near the axis of the Subtropical Gyre. This change is likely the result of surface warming and/or freshening at high latitudes, where these water masses are formed before they ventilate the base of the subtropical thermocline. Isopycnals tend to deepen south of 35°S and to shoal more weakly from 35° to 20°S. These changes are consistent with a simple model response to high-latitude warming. Results from the section comparisons are put in a larger context by estimating interdecadal changes on isopycnals throughout the South Pacific Ocean. In addition, two changes consistent with a strengthened southern influence are found within the Lower Circumpolar Water from the Chatham Rise at 43°S to the Samoa Passage at 10°S. Cooling and freshening erode the top of the deep salinity maximum of the modified North Atlantic Deep Water. In the weakly stratified abyssal layer, the modified Antarctic Bottom water cools by about 0.025°C.

1. Introduction

Ocean properties below the seasonal thermocline vary on interannual and longer timescales. These variations have been most thoroughly studied in the North Atlantic Ocean and its surrounding marginal seas, where the temporal and spatial distribution of hydrographic data is densest. Levitus (1989) includes a review of the pertinent literature as well as work on differences of intermediate-depth potential temperature (θ) and salinity (S) in the North Atlantic Ocean between 1955–59 and 1970–74. Decadal variations in the properties of the North Atlantic Deep Water are also well documented (Lazier 1988). More recent comparisons of repeat hydrographic sections in the North Atlantic Ocean show evidence for deep cooling in the eastern Subpolar Gyre between 1962 and 1981 (Read and Gould 1992). In contrast, a trend toward deep warming is apparent in repeat hydrographic sections across the subtropics from 1957 to 1981 to 1992 (Roemmich and Wunsch 1985; Parilla et al. 1994). Analysis of trends in hydrographic data throughout the North Atlantic from 1957 to 1981 (Antonov 1993) supports the conclusions drawn from repeat sections in the Subpolar and Subtropical Gyres.

One of the few places outside the North Atlantic Ocean where decadal subsurface variability is reported through comparisons of repeat hydrographic sections is the southwest Pacific Ocean. Transpacific zonal hydrographic sections at 43°S and 28°S were first occupied during the SCORPIO Expedition in 1967 (Stommel et al. 1973). The portions of these sections located in the Tasman Sea, just east of Australia, were reoccupied in 1990 and 1991, allowing comparisons between the new and historical data (Bindoff and Church 1992). A depth-averaged warming below the mixed layer at both latitudes results in an overall isopycnal deepening, which in turn gives a sea level increase of 2–3 cm, owing to

*Pacific Marine Environmental Laboratory Contribution Number 1708.

†Joint Institute for Study of the Atmosphere and Ocean Contribution Number 380.

Corresponding author address: Dr. Gregory C. Johnson, NOAA/PMEL, 7600 Sand Point Way NE, Bldg. 3, Seattle, WA 98115-0070. E-mail: gjohnson@pmel.noaa.gov

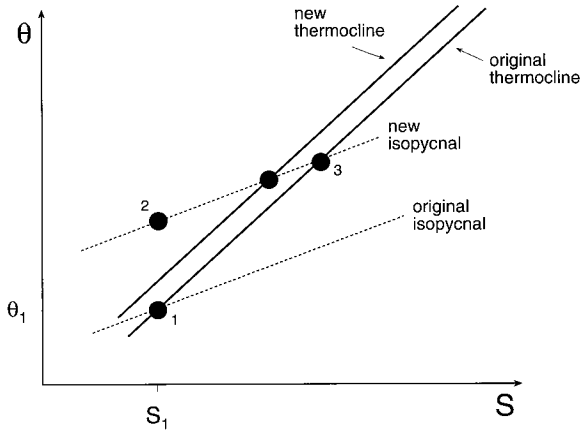

FIG. 1. Schematic showing how surface warming at water-mass formation regions can cause cooling and freshening along isopycnals in the ocean interior downstream (after Church et al. 1991; their Fig. 1). Originally, water in the near-surface formation region has certain properties (1 on the original isopycnal). Surface warming in the formation region causes ventilation to occur at a new density (2 on the lighter new isopycnal). Isopycnal mixing between this newly ventilated water at 2 with original interior water at 3 shifts the θ–S curve (original thermocline) to one that is colder and fresher along isopycnals (new thermocline).

a dynamic height change. The Bindoff and Church (1992) analysis also indicates that the Subantarctic Mode Water (SAMW) and Antarctic Intermediate Water (AAIW) underwent cooling and freshening on neutral surfaces (γ_n; Jackett and McDougall 1997). A more involved analysis of the 43°S repeat sections shows that the changes on γ_n surfaces about the SAMW are primarily accomplished by high-latitude surface warming in the formation region of this water mass, whereas those about the AAIW are the result of high-latitude surface freshening (Bindoff and McDougall 1994). These water masses play an important role in the thermohaline circulation, ventilating the base of the subtropical thermocline.

It is not intuitive that surface warming and/or freshening at the high-latitude formation regions of the SAMW and AAIW would cause cooling and freshening on interior γ_n surfaces in the southwest Pacific. The argument is outlined in Church et al. (1991). Bindoff and McDougall (1994) present refinements and outline the different effects that surface warming or freshening have for all possible interior θ–S curves. Since this concept is central to the analysis here, the most relevant case is restated. In most of the subtropical and tropical ocean, from the salinity maximum at or near the ocean surface to the salinity minimum characteristic of most intermediate waters, S and θ both decrease with increasing depth and density, giving a familiar curve (Fig. 1; original and new thermocline). Increased surface warming at high latitudes decreases the density of the subducted water masses (from point 1 on the original isopycnal to point 2 on the new isopycnal). Isopycnal mixing of this newly ventilated water (point 2) with the original thermocline water in the ocean interior (point 3) shifts the θ–S relation to colder and fresher values on the new isopycnal (dotted line). If increased surface warming occurs over a significant range of latitudes, hence surface temperatures and densities, a large portion of the θ–S curve shifts (from original thermocline to new thermocline). This change is coupled with warming along depth surfaces. Increased surface freshening from precipitation or ice melt at high latitudes has a similar effect on γ_n surfaces where θ and S both decrease with increasing depth and density but results in freshening on depth surfaces. In regions such as parts of the southeast Pacific, where S increases with depth, the effect of high-latitude increased surface warming is a warming on both γ_n and depth surfaces, and so on (Bindoff and McDougall 1994).

Variability in the Lower Circumpolar Water (LCPW) entering the North Pacific through the Samoa Passage is also documented (Johnson et al. 1994). Data taken in 1968, 1987, and 1992 suggest that the lighter LCPW component, characterized by a salinity maximum and referred to here as modified North Atlantic Deep Water (NADW), has variable water properties and transport through the passage. The denser LCPW component, characterized by near-bottom coldness and freshness, and referred to here as modified Antarctic Bottom Water (AABW), appears to exhibit less transport variability.

2. Data

The tendency in planning recent hydrographic sections has been to favor refining geographical coverage over reoccupying historical sections. Therefore, there are very few places outside of the North Atlantic Ocean where high quality hydrographic sections have been repeated. Two sets of such sections were made 23 yr apart in the Tasman Sea, and their differences have been studied extensively (Bindoff and Church 1992; Bindoff and McDougall 1994). Here we study the only other two such sets in the South Pacific Ocean of which we are aware. One set overlaps for 60° latitude along 170°W, and the other set overlaps for 11° longitude along 35°S (Fig. 2). The years in which the data were taken are similar to those for the Tasman Sea (Bindoff and Church 1992; Bindoff and McDougall 1994) and Samoa Passage (Johnson et al. 1994) studies. To put the changes observed in the SAMW and AAIW with these sections into a basin-wide context, we compare all available data taken in the South Pacific Ocean since 1987 (mostly high quality data from the World Ocean Circulation Experiment, or WOCE) to historical data of mixed quality from 1965 to 1974 on an appropriate γ_n surface. Since uniformly high quality data (the section data) are necessary to study the more subtle differences in the modified NADW and AABW, the changes observed there cannot be set in a wider context.

A meridional hydrographic section with high quality data was occupied along 170°W during the Southern

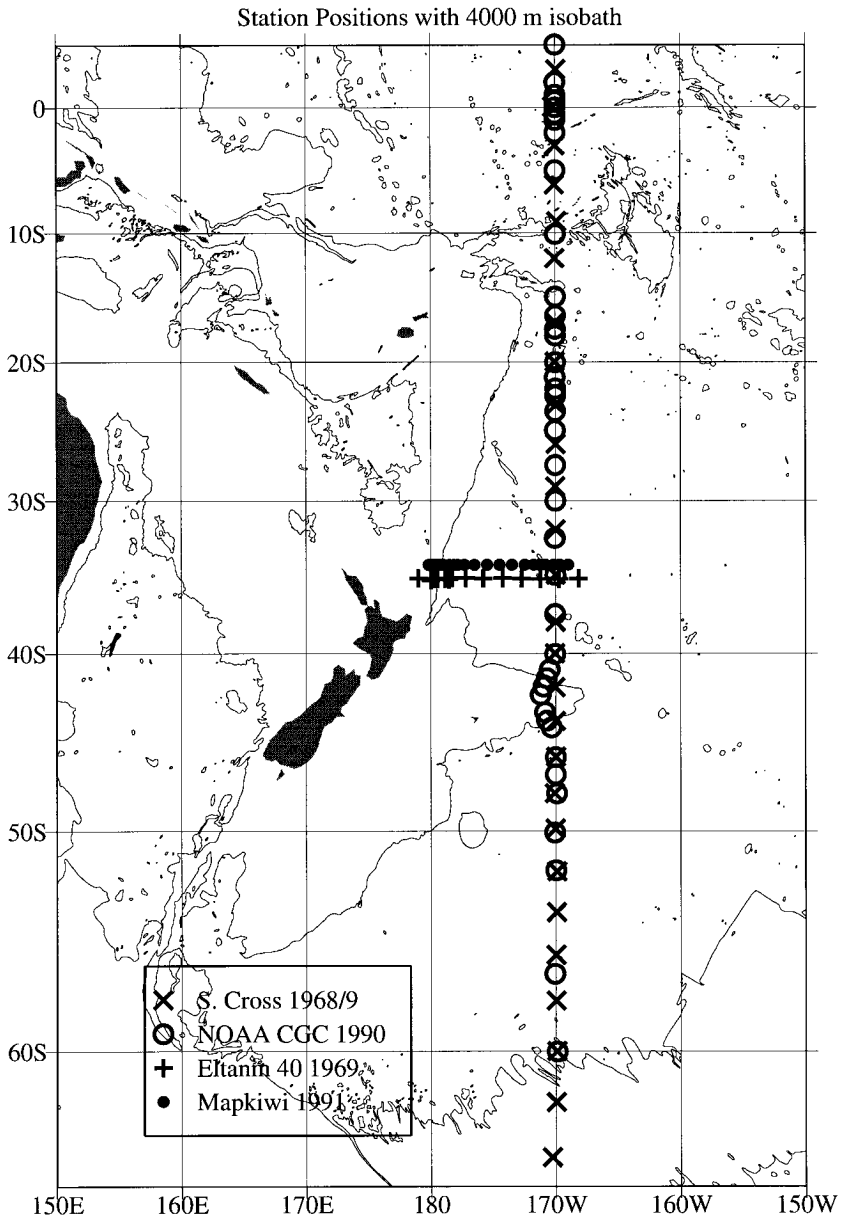

FIG. 2. Station positions of the Southern Cross section along 170°W in 1968/69 (crosses), the NOAA Climate and Global Change section along 170°W in 1990 (open circles), the *Eltanin* 40 section along 35° 15′S (pluses) and the Mapkiwi section along 34° 20'S (filled circles). The 4000-m isobath (solid line; IOC et al. 1994) shows where cruises cross the Chatham Rise (43°S) and the Samoa Passage (10°S).

Cross cruise in December 1968 and January 1969 (Horibe 1970). Twenty-four full-depth stations were taken from 60°S to the equator (Fig. 2). The Nansen bottle data are thought to be accurate to better than ±0.5% in depth, ±0.005°C in θ, and ±0.003 ppt in S. The section was repeated along the same nominal longitude by NOAA researchers in February to April 1990 (McTaggart et al. 1993). Thirty-six stations were made along the line from 60°S to the equator, with data taken from the surface to various depths. Twenty-three of these stations had full-depth casts. The CTD data are thought to be accurate to better than ±0.1% in pressure, ±0.005°C in θ, and ±0.005 pss in S. All quantities are calculated from the 1-dbar CTD data and then filtered with a 10-dbar 1/2-width Hanning filter.

A zonal hydrographic section was occupied along 35° 15′S during USNS *Eltanin* cruise 40 in September–October 1969 (Gordon and Molinelli 1975). Fourteen stations were made from 179°E to 168°W (Fig. 2). The Nansen bottle data have accuracies similar to those from

the Southern Cross cruise, except the salinities are probably only accurate to ±0.01 ppt. This zonal section was reoccupied along nearly the same latitude, 34° 20′S, during the Mapkiwi expedition in March 1991 (Moore 1994). Twenty-two full-depth stations were taken between 180° and 169°W. The Mapkiwi CTD pressure and θ data are just as accurate as those measured along 170°W. However, S is somewhat more noisy, though accurate in an overall fashion. All properties are calculated using the 1-s CTD data and then filtered with a 42-s (about 50-dbar) 1/2-width filter to remove the effects of the salinity noise.

A careful examination of all four datasets used here is made where they intersect at 35°S, 170°W. This comparison shows that salinity data from the 1969 *Eltanin* 40 section at 35°S, 170°W are about 0.006 pss fresher than those from the other three sections on θ surfaces between the salinity minimum of the AAIW and the salinity maximum of the modified NADW. This interval contains the oldest and most horizontally homogenous portion of the water column, the modified North Pacific Deep Water (NPDW), where water-mass variability should be, and is, at a minimum (Warren 1973). The other three sections agree there to within about 0.002 pss, somewhat less than their estimated accuracies. A comparison of the Wormley Standard Seawater batches used to standardize the salinity measurements on the four cruises shows that none have reported offsets (Mantyla 1987) large enough to account for the discrepancy of the *Eltanin* 40 data. This discrepancy is large enough to change conclusions regarding the observed variability in the modified NADW and AABW. Thus, while its origin is unclear, the discrepancy is removed in this analysis by adding an 0.006 offset to the *Eltanin* 40 salinity measurements.

Bindoff and McDougall (1994) have shown that the most thorough diagnosis of water-mass changes results from an examination of changes on depth and γ_n surfaces. For this analysis, means and differences of the sections are computed on both depth and γ_n. For the purposes of comparison it is useful to map data from each pair of sections to identical grids. The data and derived properties from each station are first interpolated to two sets of standard levels, one for depth and one for γ_n. The results of this first step are saved for obtaining average differences and estimating their confidence limits. The mean differences between sections over a desired latitude or longitude range are estimated as the areas of polygons enclosed by the data points from both sections plotted against latitude or longitude divided by the latitude or longitude range. The confidence limits of mean differences are then derived using a delete-one jackknife variance (Thompson and Chave 1991), which assumes that each station provides an independent measurement on each surface. The data and derived properties from all the stations on a given section are also interpolated to standard latitudes (0.5° intervals) or longitudes (0.2° intervals) at each level to display vertical sections of means and differences. A spline designed to avoid introducing spurious extrema is used for the interpolation in the vertical and the horizontal (Akima 1970).

Changes of θ and S on γ_n surfaces are statistically more robust than those on depth surfaces. This difference arises because isopycnal heave from a variety of time and space scales introduces noise in θ and S differences computed on depth surfaces. This heave can be the result of long-term changes, but other agents include mesoscale eddies, internal waves, and current meanders. Changes of θ and S on γ_n surfaces are more robust because noise from isopycnal heave is eliminated. In addition, depth differences of γ_n surfaces quantify isopycnal movements in the ocean interior, outside of the surface and bottom mixed layers. Hence the discussion of repeat section differences focuses on the more robust changes on γ_n surfaces.

To put the large changes seen around the SAMW and AAIW with the repeat sections into a larger context, mean property and property-difference maps are also shown on $\gamma_n = 26.8$ kg m^{-3}, just above the SAMW stratification minimum, where the sections show large differences on γ_n surfaces. These maps are made using hydrographic data collected since 1987 (mostly WOCE data) and historical hydrographic data collected from 1965 to 1974. Properties on this surface are objectively mapped (Gandin 1965) assuming a Gaussian covariance with horizontal correlation scales of 5° lat and long and an error-to-signal energy of unity, relaxing to a Gaussian mean estimated using the same correlation scales in data-poor regions. The mean property maps use both datasets. To make the property-difference maps, first all historical stations within 110 km of each recent station are found. Then the median differences between properties of each recent station and all nearby historical stations are found and objectively mapped.

3. Water-mass structure in the southwest Pacific Ocean

The vertical section of the mean depths of γ_n surfaces along 170°W (Fig. 3) contains information on water masses and the general circulation in the region, but inverse in appearance to a conventional vertical section of density or temperature [see Reid (1986) for a conventional presentation of the Southern Cross cruise data]. The mean depth of γ_n surfaces decreases south of 48°S throughout the water column, showing the surface-intensified, bottom-reaching, eastward currents in the Antarctic Circumpolar Current. The closely spaced (400–800 m) depth contours at $\gamma_n \sim 27.1$ kg m^{-3} just north of 48°S reveal the pycnostadt of the SAMW, which ventilates the waters at the base of the subtropical thermocline. The widely spaced (200–600 m) depth contours tilting up between 35° and 20°S in waters lighter than $\gamma_n \sim 27.1$ kg m^{-3} mark the eastward flowing portion of the subtropical thermocline. The meridional

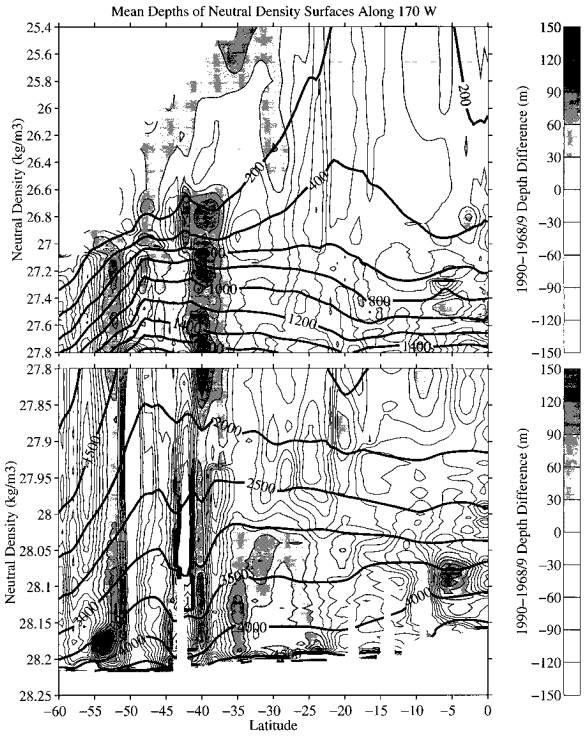

FIG. 3. Vertical section of depth means and differences on neutral (γ_n) surfaces along 170°W using the 1990 and 1968/69 data. The top panel shows densities from about 200 m of the sea surface to a mean depth of about 1500 m. The bottom panel shows the deeper densities on an expanded vertical scale. Mean depth contours (thick lines) are at 200-m intervals in the top panel and 500-m intervals in the bottom panel. Depth difference contours of 1990 – 1968/69 (thin lines) are at 30-m intervals in both panels. Shaded areas show where isopycnals have deepened over the 21-yr interval.

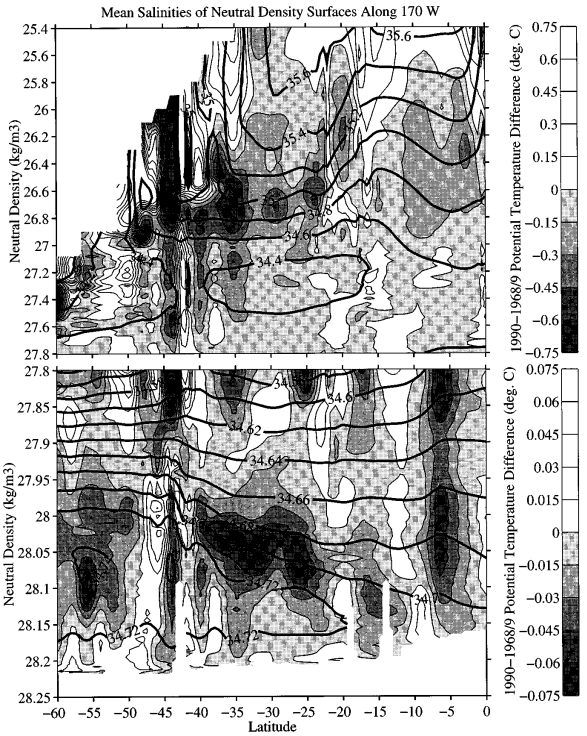

FIG. 4. Vertical section of salinity means and θ differences on γ_n along 170°W using the 1990 and 1968/69 data. The two panels are analogous to those in Fig. 3. The mean salinity contours (thick lines) are at 0.2 pss intervals in the upper panel and 0.02 pss intervals in the lower panel. Here, θ difference contours of 1990 – 1968/69 (thin lines) are at 0.15°C intervals in the upper panel and 0.015°C intervals in the lower panel. Shaded areas show where water has cooled (and freshened) on γ_n over the 21-yr interval.

maximum of depth on the lighter γ_n surfaces near 20°S marks the axis of the Subtropical Gyre. In the denser waters, below $\gamma_n \sim 27.95$ kg m^{-3}, the dynamic signature of the deep western boundary current rounding the Chatham Rise is visible at 43°S in the decreasing depths of γ_n surfaces toward the Rise on both sides. This bottom-intensified current flows northeastward against the southern side of the rise and then northwestward on the northern side of the rise before continuing north along the Tonga–Kermadec Trench (Warren 1973). Near-bottom stratification is weak in the modified AABW, as reflected by the closely spaced 4500-m and 5000-m depth contours. This dense bottom water of southern origin becomes lighter as it moves equatorward.

Two water masses of interest in this study are indicated by the extrema in the mean salinity values (Fig. 4). The fresh tongue characteristic of AAIW at $\gamma_n \sim$ 27.3 kg m^{-3} becomes a strong vertical minimum near 48°S, at the northern edge of the Subantarctic Zone, from whence it spreads below the saltier central water of the subtropical thermocline. This salinity minimum decays substantially by 20°S, north of the axis of the Subtropical Gyre. Well below the AAIW is the salinity maximum that marks the core of the modified NADW. This maximum is strongest in the Antarctic Circumpolar Current, starting at $\gamma_n = 28.07$ kg m^{-3}. It decays and shifts to a denser γ_n north of the Chatham Rise (40°S). It finally disappears as a local maximum by grounding north of the Samoa Passage (10°S). The fresher (and colder) water below the deep salinity maximum is modified AABW. These two water masses make up the LCPW, which flows north in the deep western boundary current, ventilating the abyssal Pacific Ocean.

4. Differences in the Subantarctic Mode and Antarctic Intermediate Waters

Differences of θ on γ_n show a large region of pronounced cooling (Fig. 4) from $\gamma_n \sim 26.5$ kg m^{-3} to $\gamma_n \sim 27.5$ kg m^{-3}. This range starts above the stratification minimum of the SAMW ($\gamma_n \sim 27.1$ kg m^{-3}; Fig. 3), and ends below the salinity minimum of the AAIW ($\gamma_n \sim 27.3$ kg m^{-3}; Fig. 4). This cooling (and freshening) on γ_n surfaces is strongest at $\gamma_n \sim 26.8$ kg m^{-3} near 48°S, the northern edge of the Subantarctic Zone, where peak values exceed −1.0°C, but it extends to about 20°S, near the axis of the Subtropical Gyre. Mean differences

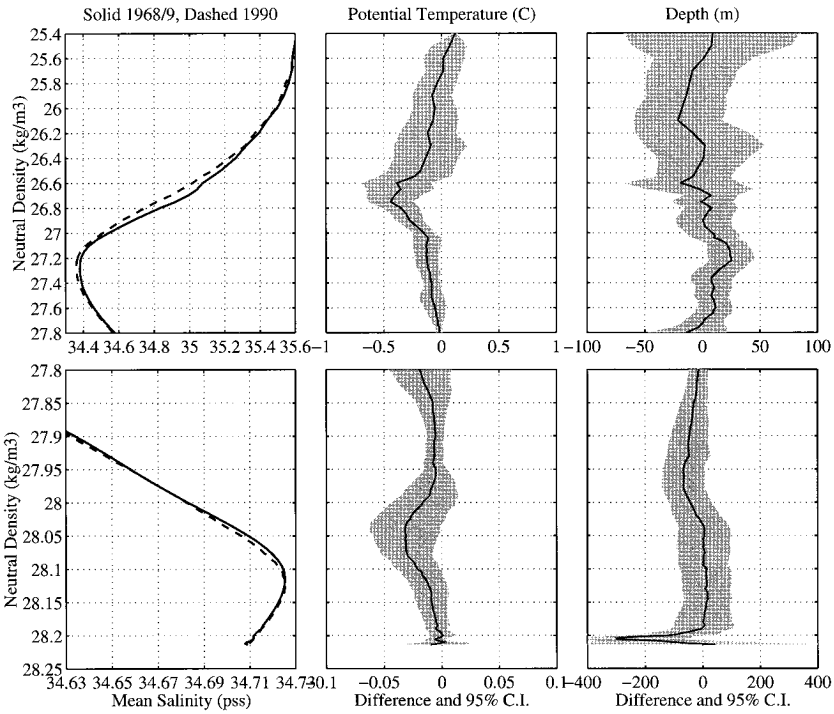

FIG. 5. Mean S curves on γ_n (left panels; solid line 1968/69, dashed line 1990) along 170°W from the start of the Antarctic Intermediate Water (AAIW) salinity minimum at 48°S to the axis of the Subtropical Gyre at 20°S. Differences for the same latitude range (solid lines), 1990 – 1968/69, with 95% confidence intervals (shaded areas) for θ and depth (middle and right panels, respectively). Positive depth differences indicate deeper isopycnals in 1990 than in 1968/69. Only data below a depth of 150 m are used, to avoid seasonal variability in the upper water column. Top and bottom panels follow the same density interval selection used in Figs. 3 and 4.

from 48° to 20°S are estimated from the raw data on γ_n below 150 m, giving a mean cooling of -0.4°C at $\gamma_n = 26.8$ kg m^{-3}, with differences significantly different from zero within a 95% confidence interval from $\gamma_n = 26.6$ kg m^{-3} to $\gamma_n = 27.5$ kg m^{-3} (Fig. 5). The mean differences for the 35°S section (from the date line to 169°W) are significant over a similar γ_n range to those along 170°W, with a peak of nearly -0.8°C at $\gamma_n = 26.8$ kg m^{-3} (Fig. 6). In both sections, these θ changes are linked through the definition of γ_n to a decrease in salinity (see Fig. 1). Changes are largest above the salinity minimum of the AAIW, but extend below it (Figs. 5 and 6).

In the Tasman Sea, a similar cooling and freshening on γ_n surfaces between sections, measured at times similar to those analyzed here, occurred with isopycnal deepening. This combined signal was attributed to the effects of surface warming at the high-latitude formation region of the SAMW and surface freshening at the higher-latitude formation region of the AAIW (Bindoff and Church 1992; Bindoff and McDougall 1994). Cooling and freshening are found on γ_n surfaces along 170°W, and it appears that isopycnals are also deepening south of 35°S, whereas they shoal farther to the north (Fig. 3). Thus, while the net difference in depths of isopycnals from 48° to 20°S is a barely significant 25-m deepening, centered at $\gamma_n = 27.75$ kg m^{-3} (Fig. 5), this is the sum of significant deepening of around 50 m in the top 2000 m south of 35°S, and slightly smaller but still significant shoaling in the top 3000 m north of 35°S (Fig. 3). The 35°S section-average differences, being located near the node of the depth changes observed along 170°W, show no coherent changes in isopycnal depth above the bottom water (Fig. 6). A simple model of the oceanic response to high-latitude surface warming suggests cooling and freshening will occur on outcropping isopycnals. At the same time isopycnals will deepen at high latitudes and shoal at lower latitudes in response to this change in forcing (Church et al. 1991). All the changes described above (and immediately below) are consistent with these model results.

To put these results into a larger context, property mean and difference maps are shown for the South Pacific on $\gamma_n = 26.8$ kg m^{-3} (Figs. 7–10). Maps are constructed using only data from the two periods studied. The recent period includes all available data since 1987, mostly WOCE data. The older period includes data collected from 1965 to 1974, a decade when a fairly large number of stations were taken in the region. The mean depth of this surface (Fig. 7) reveals the bowl of the

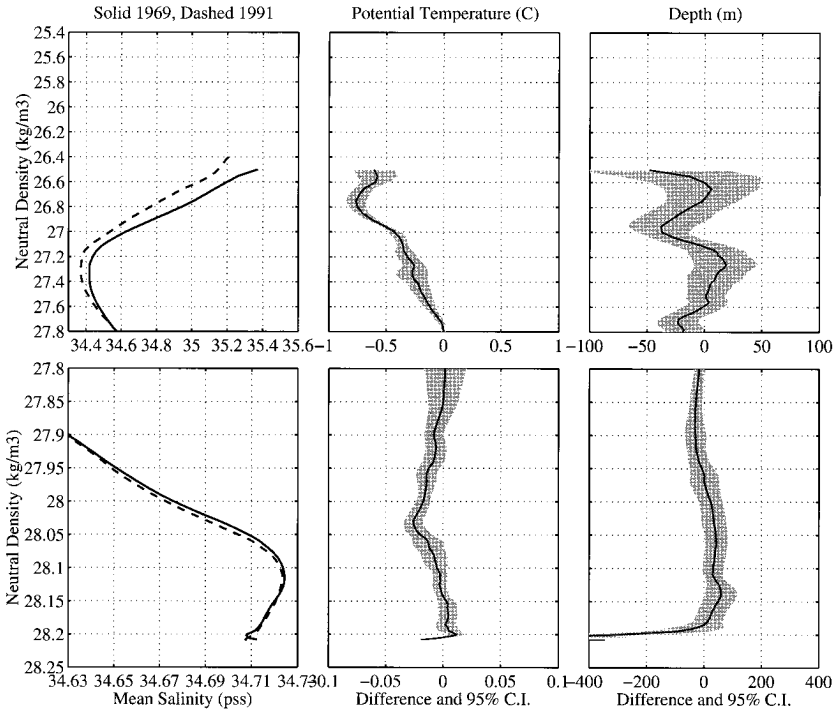

FIG. 6. Mean S curves on γ_n (left panels; solid line 1969, dashed line 1991) along 35°S from 180° to 169°W. Differences for the same latitude range (solid lines), 1991 – 1969, with 95% confidence intervals (shaded areas) for θ and depth (middle and right panels, respectively). Only data below a depth of 150 m are used, to avoid seasonal variability in the upper water column. Top and bottom panels follow the same density interval selection used in Figs. 3–5.

anticyclonic Subtropical Gyre, with a roughly zonal axis centered around 22°S; a westward-intensified southward flow to the west of its deepest point, below 550 m at 165°E; and a broad northward interior flow where it shoals to the east, reaching 400 m by 95°W. The bowl shoals northward to less than 350 m at 5°–15°S, indicating westward flow, and southward to about 150 m by 45°S, resulting in eastward flow. Depth differences are computed only where data from the earlier decade are found within 110 km of data from the recent decade, which unfortunately but irremediably results in somewhat spotty coverage of the basin (Fig. 8). Coverage notwithstanding, the largest depth changes on this γ_n surface appear to occur near the southwestern end of the gyre. In this region deepening is again seen south of 30°–35°S, with some shoaling present to nearly 20°S.

The mean salinity map also reflects the influence of the anticyclonic gyre at this γ_n surface (Fig. 9). A fresh cool tongue of water first spreads northward from the far southeast Pacific Ocean and then roughly westward just north of the gyre's axis from 25°S, 105°W to 15°S, 170°E. A salty tongue originating near the terminus of

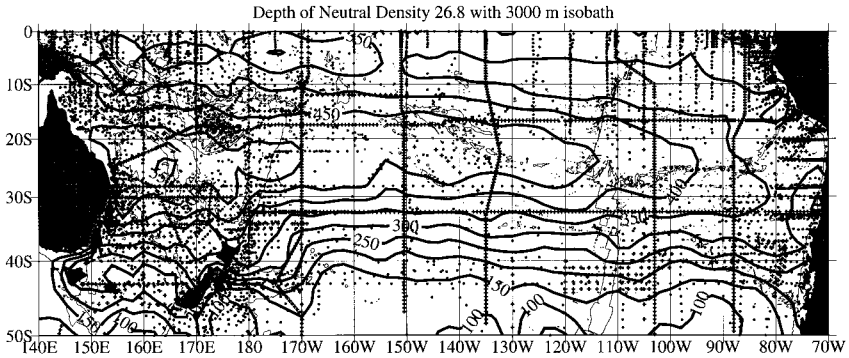

FIG. 7. Objective map of the depth of $\gamma_n = 26.8$ kg m^{-3} using hydrographic data from 1965 to 1974 (filled circles) and data from 1987 to 1996 (pluses). Depths (thick lines) are contoured at 50-m intervals. The 3000-m isobath (thin lines) is shown (IOC et al. 1994).

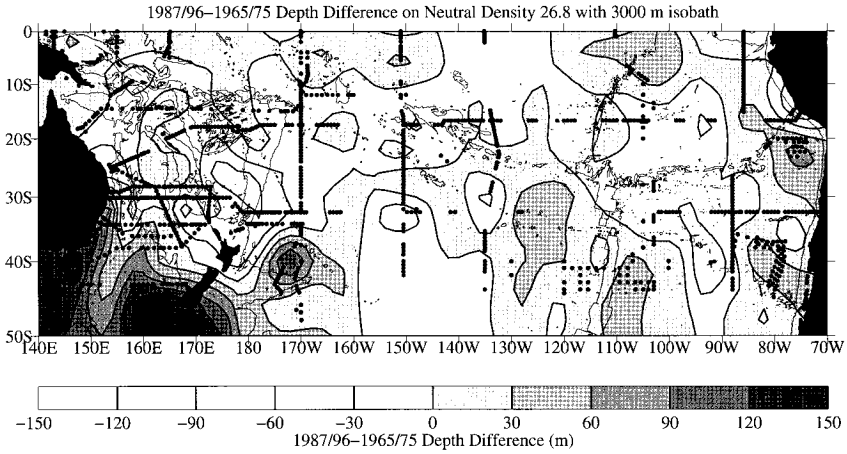

FIG. 8. Contours of depth differences between data from 1965 to 1974 and data from 1987 to 1996. Following Fig. 3, depth differences are contoured at 30-m intervals and shaded areas show where isopycnals have deepened in the 21-yr interval. Differences are computed at locations where data from the two periods are in similar locations (filled circles), as described in the text. The 3000-m isobath (thin lines) is shown (IOC et al. 1994).

the East Australia Current at 40°S, 150°E spreads roughly eastward to 30°S, 110°W, south of the gyre's axis. The θ-difference map shows an overall cooling (and freshening) on this γ_n surface (Fig. 10), which is strongest in the southwest Pacific. A conspicuous exception to this pattern is the large region of strong increase of temperature on the density surface in the southeast Pacific, where the Subantarctic Zone is at its widest and its surface water the freshest. Thus, unlike the rest of the area studied, salinity actually increases with depth in the southeast Pacific around $\gamma_n = 26.8$ kg m^{-3}. This locally different sign of the θ–S curve is such that surface warming would result in an increase of temperature and salinity on interior γ_n surfaces (Bindoff and McDougall 1994), just as observed here. Thus, the changes in the θ–S relation on this γ_n surface across the entire region, except for a small area north of New Zealand, are consonant with a high-latitude surface warming where the SAMW is ventilated, namely the Subantarctic Zone.

Significant cooling and freshening extends to a few hundred meters below the AAIW salinity minimum in the southwest Pacific Ocean (Figs. 5 and 6). The AAIW salinity minimum can be traced to surface water at even higher latitudes than that producing SAMW. The AAIW is linked to the very cold and fresh Antarctic Surface Water of the Antarctic Zone, which extends south of the Polar Front (Molinelli 1981; Piola and Georgi 1982). Because the AAIW core is an absolute salinity minimum throughout the water column everywhere north of the Subantarctic Front, high-latitude surface freshening is necessary to cool and freshen the AAIW on γ_n surfaces (Bindoff and McDougall 1994). Including sea ice in the freshwater budget allows increased surface heat flux in the Antarctic Zone to cause freshening, because such a flux would most likely result in increased sea ice melting, without a significant change in the surface water temperatures. Thus, surface warming in the Antartic Zone would freshen the Antarctic Surface Water while keeping temperatures low, which would in turn freshen

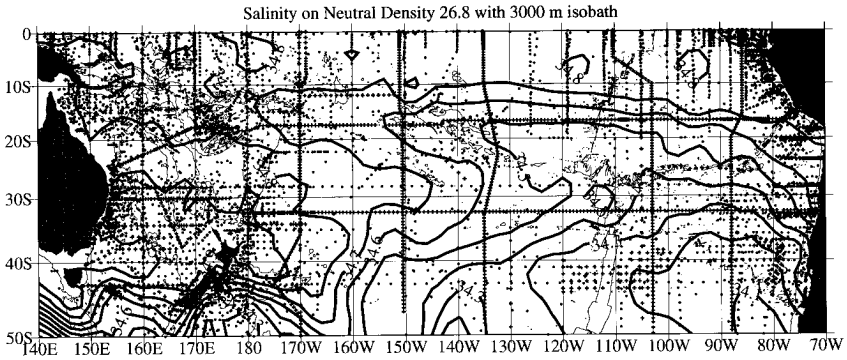

FIG. 9. Objective map of the salinity on $\gamma_n = 26.8$ kg m^{-3} using hydrographic data from 1965 to 1974 (filled circles) and 1987 to 1996 (pluses). Salinities are contoured at 0.1 pss intervals. The 3000-m isobath (thin lines) is shown (IOC et al. 1994).

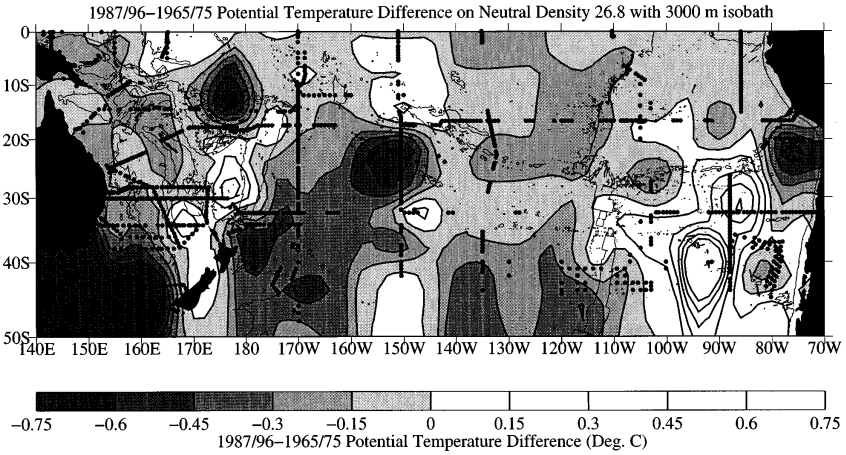

FIG. 10. Contours of θ differences between data from 1965 to 1974 and data from 1987 to 1996. Following the upper panel of Fig. 4, θ differences are contoured at 0.15°C intervals and shaded areas show where γ_n surfaces have cooled (and freshened) in the 21-yr interval. Differences are computed at locations where data from the two periods are in similar locations (filled circles), as described in the text. The 3000-m isobath (thin lines) is shown (IOC et al. 1994).

the salinity minimum of the AAIW to the north. Increased precipitation at these high latitudes could also account for this change.

5. Differences in the Lower Circumpolar Water

The LCPW is made up of NADW and AABW, modified within the Antarctic Circumpolar Current (Reid 1986). Some of the LCPW flows northward in a deep western boundary current along the Tonga–Kermadec Ridge, ventilating the abyssal Pacific (Warren 1973). A pronounced cooling and freshening on neutral density surfaces is observed just above the deep salinity maximum that indicates the modified NADW along 170°W (Figs. 4 and 5; $\gamma_n \sim 28.1$ kg m^{-3}). The changes trend from $\gamma_n \sim 28.02$ kg m^{-3} near 40°S, just north of the Chatham Rise, toward $\gamma_n \sim 28.13$ kg m^{-3} near 10°S, the Samoa Passage. The θ differences reach a peak of -0.07°C, a -0.01 salinity difference, near the center of the sections along 170°W (Fig. 4). In addition to weakening, the salinity maximum of the modified NADW becomes denser (Figs. 5 and 6). The mean θ difference in the subtropics peaks around $\gamma_n \sim 28.05$ kg m^{-3} (Fig. 5) at -0.03°C. The North Pacific Deep Water resides slightly shallower, at $\gamma_n \sim 27.9$ kg m^{-3}, where little change is seen over the two decades. This result is to be expected for this water mass, which has a residence time of centuries. Below the salinity maximum is the modified AABW, where there is also little change in the θ–S relation. This finding is not necessarily expected, since this water mass is probably renewed at least as quickly as the modified NADW. This same pattern is seen in the zonal sections along 35°S (Fig. 6), which extend from the Tonga–Kermadec Ridge to just beyond 170°W.

The origin of the salinity maximum is ultimately in the deep-water formation regions in the North Atlantic, such as the Norwegian–Greenland and Labrador Seas. Deep-water mass properties in the Labrador Sea exhibit decadal changes of as much as 0.7°C and 0.08 pss in salinity on density surfaces (Rhines 1994), nearly an order of magnitude greater than those observed here. A century is a reasonable estimate for the time it might take these differences to travel at 1.4 cm s^{-1} from the North Atlantic to the Samoa Passage (Johnson et al. 1994). In addition, the salinity maximum is modified substantially through contact with other water masses during its travel from the North Atlantic to the South Pacific (Reid and Lynn 1971). Variability in the adjacent water masses or the circulation path could be responsible for the changes observed. The uncertainties in the travel time, the pathway, and the mixing history of the water mass make it difficult to link the observed changes near the deep salinity maximum in the South Pacific to variability at the source region in the North Atlantic.

At these speeds water might take about a decade to transit from 40° to 10°S along the Tonga–Kermadec Ridge. Thus, the time interval between the repeat sections at 35°S and 170°W might be long enough for a signal with a decadal timescale to move completely through the area, in which case the variability would be undersampled. However, the large spatial scales over which the anomalies are seen suggest the observed differences may not be too badly aliased in this instance. These changes are of the same sign and magnitude as those seen at 10°S in the Samoa Passage between 1987 and 1992 (Johnson et al. 1994). Northward advection from the nose of the high signal seen near 20°S in 1990 to the Samoa Passage at 10°S in 1992 at a speed of around 0.014 m s^{-1} could link these two patterns. This

speed is somewhat less than the mean speeds estimated for the deep western boundary current transporting water northward just east of the Tonga–Kermadec Ridge (Whitworth 1994) but is probably reasonable in that Lagrangian advection of a climate anomaly is likely to be slower than Eulerian current values owing to the influence of eddies and recirculations.

While the modified AABW does not show any appreciable variability of water mass properties on γ_n, there is a strong shoaling of near-bottom isopycnals, with peak mean differences of 300 m at 170°W and 500 m at 35°S (Figs. 3, 5, and 6). This shoaling is the result of the weakly stratified bottom water below 4500 m becoming colder (hence denser) by 0.02 ± 0.01°C between the Chatham Rise and the Samoa Passage at 170°W and cooling by 0.030 ± 0.005°C along 35°S. Data taken in 1987 and 1992 across the Samoa Passage at 10°S are about 0.02°C cooler in this bottom layer than data taken in 1968. This subtle but significant result is not noted by Johnson et al. (1994), but it is revealed by an increase over time in cross-sectional area of the coldest water in their water-mass censuses of the Samoa Passage (their Fig. 3). The meridional gradient of bottom θ in the southwest Pacific is -5×10^{-8} °C m^{-1}. Hence the 0.025°C cooling over 21 years is equivalent to a northward advance of 5° lat of bottom potential isotherms, a speed of 1 mm s^{-1}. The origin of this change is uncertain, but it does represent a stronger influence of modified AABW within the LCPW in the later surveys. This change could be the result of a larger transport of modified AABW, or a reduction in the modified NADW component of the LCPW.

6. Discussion

Two previous studies of South Pacific Ocean internal variability focused on SAMW and AAIW in the Tasman Sea (Bindoff and Church 1992; Bindoff and McDougall 1994). Another study examined variability of deep and bottom water in the Samoa Passage (Johnson et al. 1994). The present study uses the only other available high quality repeat hydrographic sections in the South Pacific to expand the regional coverage of these previous studies (Fig. 2). A remarkably large horizontal extent is found for the cooling and freshening observed on γ_n surfaces around the SAMW and AAIW between 1968/69 and 1990/91 at both 170°W and 35°S. This result proves that these changes, first noted in the Tasman Sea, have a broad geographical distribution in the subtropical southwest Pacific Ocean (Figs. 4, 5, and 6). Cooling and freshening on density surfaces is also found in a large region just above the salinity maximum of the modified NADW, most strongly between 40° and 20°S (Fig. 4). This same change also reduces the temperature of the salinity maximum (Figs. 5 and 6). These same patterns were observed between 1987 and 1992 in the much smaller area of the Samoa Passage at 10°S (Johnson et al. 1994). In addition, the bottom θ of the modified AABW cooled all along 170°W (Figs. 3 and 5), at 35°S (Fig. 6), and at the Samoa Passage (10°S). A reduction in strength of the modified NADW and an increase in strength of the modified AABW flowing north into the Pacific over the two-decade interval are likely responsible for these changes. Whether these changes are owing to variations in LCPW volume transport, water properties in the formation regions, some other influence, or a combination of effects is not resolved by these data.

The changes in the SAMW and AAIW are consistent with the response of a simple model to decadal timescale surface warming and/or freshening at the high-latitude formation regions of SAMW and AAIW (Church et al. 1991). In contrast, a recent study of sea surface temperature, wind stress, atmospheric pressure, and sea ice extent shows a coherent pattern of interannual variability, which takes 8–10 yr to propagate around the Southern Ocean, named the Antarctic Circumpolar Wave by White and Peterson (1996). The amplitude of the sea surface temperature anomalies in the wave is over 1°C peak to peak, with a period of 4–5 yr. This amplitude may be large enough to account for the changes seen in the repeat sections, in which case an interval of two decades between measurements might badly alias any subsurface signatures of this phenomenon.

However, the large spatial extent of the changes in the mode, intermediate, deep, and bottom waters suggests that they all occurred over a decadal timescale. In addition, an apparent age distribution along the CGC 90 section at 170°W can be inferred from CFC-11 measurements. Their distribution suggests that the timescales for ventilation are fairly long in both the SAMW and AAIW. Apparent ages can be calculated from partial pressures of CFC-11. Along $\gamma_n = 26.8$ kg m^{-3}, these ages range from over 5 years at 48°S to over 20 yr at 20°S. Along $\gamma_n = 27.4$ kg m^{-3}, the progression is from over 25 yr to nearly 40 yr. On both of these surfaces, the pattern of cooling and freshening is nearly uninterrupted from 48° to 20°S and over a 15-yr time period. This interval is long enough to incorporate three full cycles of sea surface temperature anomaly carried by the Antarctic Circumpolar Wave. The long timescales inferred from the CFC-11 measurements together with the large spatially coherent pattern of water mass changes in the SAMW and AAIW suggest that the observed differences are the result of an integration of variations in surface forcing over timescales longer than 5 yr.

One design criterion adopted for the WOCE sections was refinement of geographical coverage rather than reoccupation of previous high quality hydrographic sections. This criterion makes a thorough study of water mass changes difficult. However, the comparison of WOCE data to a set of mixed quality hydrographic data on $\gamma_n = 26.8$ kg m^{-3} shows a sign reversal of θ differences in the southeast and southwest Pacific. This

intriguing result could plausibly be the response of an ocean with vertical salinity gradients of opposite sign in the two regions to a large-scale high-latitude surface warming. Analagous basin-wide study in the LCPW is impossible owing to the need for more accurate salinity measurements. A reoccupation of the 1967 SCORPIO section at 43°S from New Zealand to Chile would allow for a more rigorous transpacific evaluation of water-mass changes throughout the water column.

Acknowledgments. This work was funded by the Climate and Global Change Program through the NOAA Office of Global Programs. We thank Thomas Whitworth III for allowing us to use the Mapkiwi data along 35°S prior to their publication. John Bullister kindly provided the CFC data from the C&GC 1990 cruise. The maps of property differences on neutral surfaces could not have been made without the hard work of the many colleagues involved in the WOCE program in the South Pacific Ocean. Thanks for their permission to use the WOCE data for this purpose. Nathan Bindoff and two anonymous reviewers also provided comments and criticism that greatly improved the manuscript.

REFERENCES

Akima, H., 1970: A new method of interpolation and smooth curve fitting based on local procedures. *J. Assoc. Comput. Mach.,* **17,** 589–602.

Antonov, J. L., 1993: Linear trends of temperature at intermediate and deep layers of the North Atlantic and North Pacific Oceans: 1957–1981. *J. Climate,* **6,** 1928–1942.

Bindoff, N. L., and J. A. Church, 1992: Warming of the water column in the southwest Pacific Ocean. *Nature,* **357,** 59–62.

——, and T. J. McDougall, 1994: Diagnosing climate change and ocean ventilation using hydrographic data. *J. Phys. Oceanogr.,* **24,** 1137–1152.

Church, J. A., J. S. Godfrey, D. R. Jackett, and T. J. McDougall, 1991: A model of sea level rise caused by ocean thermal expansion. *J. Climate,* **4,** 438–456.

Gandin, L. S., 1965: Objective analysis of meteorological fields. Israel Program for Scientific Translations, English Translation No. 1373, 242 pp. [Available from U.S. Dept. of Commerce, Clearinghouse for Federal Scientific and Technical Information, 5285 Port Royal Road, Springfield, VA 22161.]

Gordon, A. L., and E. Molinelli, 1975: *USNS ELTANIN Southern Ocean Oceanographic Atlas, Cruises 4–55, June 1962–November 1970.* Columbia University, 11 pp. and 223 plates.

Horibe, Y., Ed., 1970: Preliminary report of the Hakuho maru Cruise KH-68-4 (Southern Cross Cruise), November 14, 1968–March 3, 1969, Central and South Pacific. Ocean Research Institute, University of Tokyo, Nakano-ku, Tokyo, Japan, 170 pp. [Available from Ocean Research Institute, University of Tokyo, 1-15-1, Minamidai, Nakano-ku, Tokyo 164, Japan.]

IOC, IHO, and BODC, 1994: *Supporting Volume to the GEBCO Digital Atlas.* British Oceanographic Data Centre, 70 pp. and annexes.

Jackett, D. R., and T. J. McDougall, 1997: A neutral density variable for the world's oceans. *J. Phys. Oceanogr.,* **27,** 237–263.

Johnson, G. C., D. L. Rudnick, and B. A. Taft, 1994: Bottom water variability in the Samoa Passage. *J. Mar. Res.,* **52,** 177–196.

Lazier, J. R. N., 1988: Temperature and salinity changes in the deep Labrador Sea. *Deep-Sea Res.,* **35,** 1247–1253.

Levitus, S., 1989: Interpentadal variability of temperature and salinity at intermediate depths of the North Atlantic Ocean, 1970–1974 versus 1955–1959. *J. Geophys. Res.,* **94,** 6091–6131.

Mantyla, A., 1987: Standard seawater comparisons updated. *J. Phys. Oceanogr.,* **17,** 543–548.

McTaggart, K., D. Wilson, and L. Mangum, 1993: CTD measurements collected on a climate and global change cruise along 170°W during February–April 1990. NOAA Data Rep. ERL PMEL-44, 265 pp. [Available from NOAA/PMEL, 7600 Sand Point Way NE, Seattle, WA 98115.]

Molinelli, E. J., 1981: The Antarctic influence on Antarctic intermediate water. *J. Mar. Res.,* **39,** 267–293.

Moore, M. I., 1994: CTD data from the southwest Pacific deep western boundary current: MAPKIWI-1, R. V. Rapuhia voyage 2041, February–March 1991. NZOI Physics Section Rep. 94-5, 22 pp. [Available from National Institute of Water and Atmospheric Research, P.O. Box 14901, Wellington, New Zealand.]

Parilla, G., A. Lavin, H. Bryden, M. Garcia, and R. Millard, 1994: Rising temperatures in the subtropical North Atlantic Ocean over the past 35 years. *Nature,* **369,** 48–51.

Piola, A. R., and D. T. Georgi, 1982: Circumpolar properties of Antarctic intermediate and subantarctic mode water. *Deep-Sea Res.,* **29,** 687–711.

Read, J. F., and W. J. Gould, 1992: Cooling and freshening of the subpolar North Atlantic Ocean since the 1960s. *Nature,* **360,** 55–57.

Reid, J. L., 1986: On the total geostrophic circulation of the South Pacific Ocean: Flow patterns, tracers and transports. *Progress in Oceanography,* Vol. 16, Pergamon Press, 1–61.

——, and R. J. Lynn, 1971: On the influence of Norwegian–Greenland and Weddell Seas upon the bottom waters of the Indian and Pacific Oceans. *Deep-Sea Res.,* **18,** 1063–1088.

Rhines, P., 1994: Climate changes in the Labrador Sea, its convection and circulation. *The Atlantic Climate Change Program: Proc. PI's Meeting,* Princeton, NJ, UCAR/NOAA, 85–96.

Roemmich, D., and C. Wunsch, 1985: Two transatlantic sections: Meridional circulation and heat flux in the subtropical North Atlantic Ocean. *Deep-Sea Res.,* **32,** 619–664.

Stommel, H., E. D. Stroup, J. L. Reid, and B. A. Warren, 1973: Transpacific hydrographic sections at lats. 43°S and 28°S: The SCORPIO Expedition-I. Preface. *Deep-Sea Res.,* **20,** 1–7.

Thompson, D. J., and A. D. Chave, 1991: Jackknifed error estimates for spectra, coherences, and transfer functions. *Advances in Spectral Analysis and Array Processing,* S. Haykin, Ed., Vol. 1, Prentice Hall, 58–113.

Warren, B. A., 1973: Transpacific hydrographic sections at lats. 43°S and 28°S: The SCORPIO Expedition-II. Deep water. *Deep-Sea Res.,* **20,** 9–38.

White, W. B., and R. G. Peterson, 1996: An Antarctic circumpolar wave in surface pressure, wind, temperature, and sea-ice extent. *Nature,* **380,** 699–702.

Whitworth, T., 1994: Deep flow in the Southwest Pacific U.S. WOCE Report 1994, U.S. WOCE Implementation Rep. 6, 48 pp. [Available from U.S. WOCE Office, College Station, TX 77846.]